# Observations of Tidal Flat Sedimentation within a Native and an Exotic *Spartina* Species

Barbara Proença [1,2,*], Florian Ganthy [3], Richard Michalet [1] and Aldo Sottolichio [1]

[1] EPOC UMR CNRS 5805, University of Bordeaux, Allée Geoffroy St. Hilaire, CEDEX, 33615 Pessac, France; richard.michalet@u-bordeaux.fr (R.M.); aldo.sottolichio@u-bordeaux.fr (A.S.)

[2] Department of Geology, Faculty of Science of the University of Lisbon, IDL, Bloco C6 2° piso, Campo Grande, 1749-016 Lisboa, Portugal

[3] Ifremer LER/AR, Quai du Commandant Silhouette, 33120 Arcachon, France; Florian.Ganthy@ifremer.fr

* Correspondence: bllproenca@fc.ul.pt

**Abstract:** Field measurements of bed elevation and related wave events were performed within a tidal marsh, on two cordgrass species, *Spartina anglica* (exotic) and *Spartina maritima* (native), in the Bay of Arcachon (SW France). Bed- and water-level time series were used to infer on the sediment behavior patterns from short to long term. A consistent response was found between the bed-level variation and the wave forcing, with erosion occurring during storms and accretion during low energy periods. Such behavior was observed within the two species, but the magnitude of bed-level variation was higher within the native than the exotic *Spartina*. These differences, in the order of millimeters, were explained by the opposite allocation of biomass of the two species. On the long term, the sedimentation/erosion patterns were dominated by episodic storm events. A general sediment deficit was observed on the site, suggested by an overall bed-level decrease registered within both species. However, further verification of within species variation needs to be considered when drawing conclusions. Despite possible qualitative limitations of the experimental design, due to single point survey, this work provides original and considerable field data to the understanding the different species ability to influence bed sediment stabilization and their potential to build marsh from the mudflat pioneer stage. Such information is valuable for coastal management in the context of global change.

**Keywords:** cordgrass; mesotidal lagoon; ecosystem engineering; field experiment; acoustic altimetry; sedimentation/erosion patterns

## 1. Introduction

The interactions between aquatic vegetation and the physical environment, play a major role in the evolution of coastal areas [1–6]. At the scale of an ecosystem, the erosion and accretion patterns resulting from bio-geomorphic feedbacks depend on local, short-term, sediment dynamics around or within patches of vegetated structures, where their species dependency is still poorly understood [7]. The comprehension of the underlying physics governing the formation and evolution of these coastal landscapes is necessary [8,9], as growing attention is given to ecosystem-based coastal protection solutions [10–12]. In this sense, field data provide a valuable contribution to improvements of this knowledge.

Given the substantial ecosystem functioning and services provided by tidal marshes [13], considerable attention has been given to the understanding of the feedback loop between vegetation in general, hydrodynamics and sediment dynamics, both in current- and wave-driven flows [14–22]. Indeed, an organism's efficiency to sediment trapping and stabilization by alteration of the incident physical forcing is closely related to its traits, which are species [23] and season dependent [24,25]. In particular, in the case of aquatic vegetation, the plant traits action can then be separated in aboveground and belowground effects.

The aboveground effects directly concern the vegetation aerial biomass and are dependent on specific traits, such as height, density and stiffness [5,15,17,26,27] and surface of occupation [28]. More specifically, vegetation aboveground biomass contributes to the reduction of the hydrodynamic energy [5,14,29], leading to a decrease of bottom shear stresses [17,30,31]. For example, Chen et al. [27] observed that *Spartina alterniflora* pioneer patches on the bare mudflats show considerable flow reduction ability, even better than homogenous *Spartina* cover with high biomass density, but they failed to confirm the same pattern for other types of vegetation. Such result supports the strong species dependency of the response by abiotic forces. By attenuating water velocities, more plant shoots will consequently tend to favor terrigenous sediment deposition [32–34], and specific marsh grass morphologies can further affect inorganic sediment accretion [35].

Furthermore, mechanical reinforcement of soil stability can be largely enhanced by plant root systems [36–38]. For instance, the erosion-reducing potential of species presenting root systems with different properties (diameter and length) has been shown by [39] with a field experiment in Belgium river dikes. They investigated the depth of action of five communities of plant root systems, each of them showing different properties on soil resistance to erosion and found an overall decrease of both root density and soil cohesion with depth. Erosion tests conducted in tidal flats colonized by the seagrass *Zostera noltei* [40] also showed an increase in bed sediment stabilization related to an increase in the critical shear stress for bed erosion, due to seasonally more developed root systems. The bed level variation is an important parameter for the understanding of the extent of the interactions between the vegetation, hydrodynamics and the resultant sediment motion [41]. The importance of bed level variation is due to the fact that it integrates a series of physical and biological processes that determine marsh formation. However, reliable bed level monitoring needs continuous measurements which requires expensive and difficult material to set up. Such type of measurements is scarce and valuable for numerical modelling studies.

In the Bay of Arcachon (Southwest Atlantic coast of France), salt marshes are dominated by two cordgrass species, *Spartina maritima*, a European native species, and *Spartina anglica*, a species that was introduced in the Bay in the 1980s [42]. The two species present differences in terms of traits, biomass allocation and seasonal development [43]. Given the numerous functioning values provided by salt marshes and considering the growing global change pressure they are facing, a deep knowledge of the underlying processes of marsh adaptation capacity through tidal flat colonization is needed [44]. The evolution of tidal flats into salt marsh entails an evolution of its functioning, both physically (hydrodynamics and morphology) and biologically. The processes underlying the interactions between vegetation and the incident hydrodynamic forces have been widely assessed both with field and laboratory studies. However, they mostly consider well-developed marsh vegetation, and less attention has been given to marsh vegetation at the pioneer stage. Hence, for management purposes, it is important to understand the underlying processes of the transition between the pioneer mudflat stage and marsh development. With this study, we aim at providing field observations of bed-level evolution in response to the wave action, within the two cordgrass species present in the Bay of Arcachon, in their pioneer stage.

## 2. Materials and Methods

### 2.1. Study Area

The Bay of Arcachon is a mesotidal coastal lagoon, semi-enclosed from the ocean by the Cap Ferret sandspit, located in the Bay of Biscay (south west Atlantic coast of France; Figure 1). The Bay has an equilateral triangular shape of 20 km long sides. Its mean depth is of 4.6 m [45] and 75% of the total surface corresponds to intertidal mudflats [46].
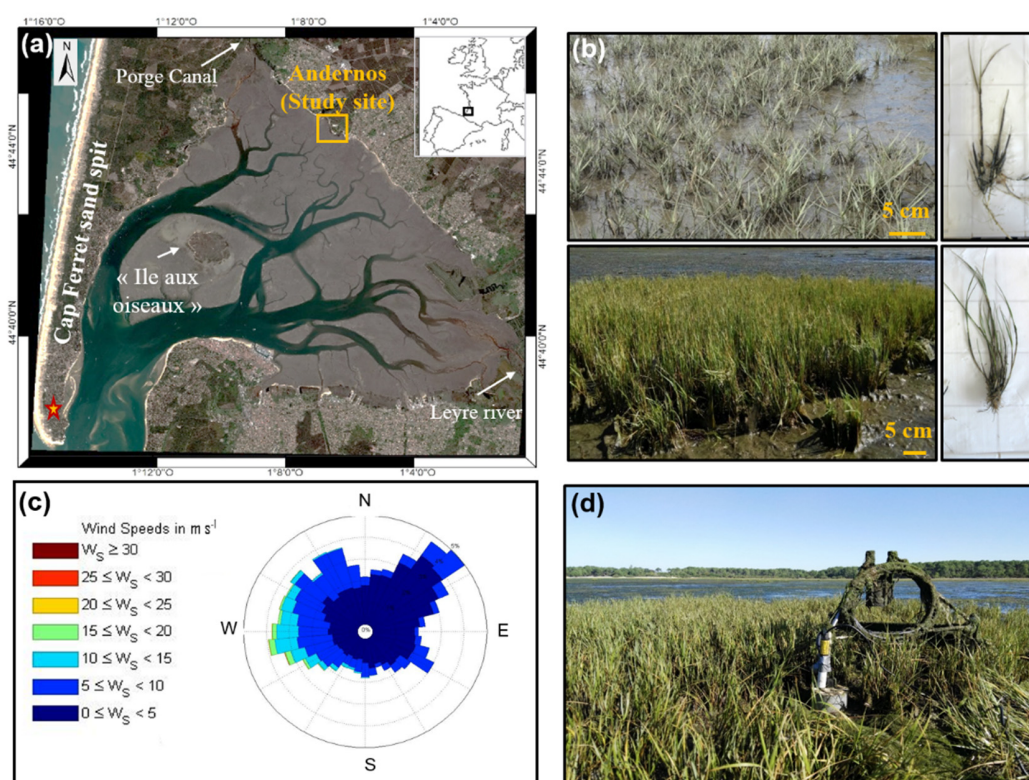
**Figure 1.** (**a**) Location of the study site of Andernos (yellow box) within the Bay of Arcachon. Red/yellow star indicates the location of the Cap Ferret's meteorological station. (**b**) Characterization of *Spartina anglica* meadow (top left) and individual plant (top right) and *Spartina maritima* meadow (bottom left) and individual plant (bottom right). (**c**) Wind rose for wind records at the meteorological station of Cap Ferret indicated in (**a**) during the period of the field experiment. (**d**) ALTUS device mounted on a structure installed within *Spartina maritima* vegetation patch.

The Cap Ferret sandspit and the presence of sand banks and shoals at the inlet strongly limit the entrance of oceanic swell, and thus, circulation inside the bay is mainly driven by tidal currents and locally generated wind waves [47]. Tides are predominantly semi-diurnal, and tidal amplitude in the lagoon ranges from 0.8 m at neap tides to 4.5 m at spring tides [48]. The general circulation in the Bay is ebb-dominated [45], which means that the lagoon mostly exports sediment [48]. The velocity of the tidal currents considerably decreases throughout the lagoon, where highest values can reach more than 2 m s$^{-1}$ at the entrance [45,49], decreasing to values between 0.1 and 0.5 m s$^{-1}$ on the intertidal zone [45,50]. The waves are wind dominated and thus closely related to the wind conditions [47]. Strongest winds come mostly from W-NW sector. Because of this wind dependency, wave heights inside the Bay are limited by the fetch, which, depends on wind direction and is strongly affected by the presence of an island in the middle of the Bay, "l'Ile aux oiseaux". Wave and wind measurements by Parisot et al. [47] inside the lagoon showed a good correlation between wind intensity and wind wave formation. More precisely, they found that winds higher than 10 m s$^{-1}$ generated waves higher than 10 cm and strongest wind events could generate waves higher than 20 cm that could reach up to 50 cm. They also verified a non-linear relationship between the increase of significant wave height and water depth and typical wave periods between 1 s and 4 s.

Many small streams discharge into the lagoon. However, the main riverine input mostly comes from two rivers: the Eyre, in the SE, and the Porge canal, on the northern limit, contributing with 73% and 24% of the total annual discharge, respectively [45,51]. This riverine discharge (and inherent sediment input) is negligible, as it is considerably lower (400 times) than the volume of incoming seawater, and the overall sediment budget in the Bay is negative [46]. At the mouth of the lagoon, the sediment is mainly composed

of coarse-grain sand [52]. At the inner tidal flats, sediment is mostly muddy, which shows the sheltered character of the internal section of the Bay.

### 2.2. Vegetation in the Bay of Arcachon

Mudflats in the Bay of Arcachon are extensively colonized by *Zostera noltei*. These seagrass meadows occupy more than 40% of the intertidal surface, and it has been demonstrated that they damp tidal currents [53] and play a major role on tidal flat sediment stabilization [40,50]. However, this species presence in the Bay is reportedly declining since the middle of the 2000s [51]. Since seagrass beds have important ecological values [54], importance is currently given to a better understanding of the factors contributing to its decline in the Bay [55].

Salt marshes in the Bay of Arcachon were initially dominated by the cordgrass species *Spartina maritima*, a native European species. In the 1980s, there was the introduction of the exotic species *Spartina anglica*, which is considered as a strong invader in several countries [42,56]. Both *Spartina* species present the same range of occupation along the intertidal profile [43]. They typically form extensive meadows along the coast, but they can also extend towards the inner Bay in isolated clonal patches, especially the exotic *Spartina*, where it co-occurs with seagrass *Zostera noltei* [57]. Even though the two cordgrass species are very similar, they present significant differences in terms of biomass allocation, where the native species favors aerial biomass, and the exotic one, on the contrary, presents a more developed root and rhizome system [43].

### 2.3. Sampling and Analysis

Field work was conducted on the tidal flat at Andernos (44.74° N, 1.12° W), located in the north eastern part of the Bay of Arcachon (Figure 1a), during a total period of 14 months, between the 28th of November 2016 and the 3rd of February 2018.

The choice of the sampling zone was determined by the presence of patches of *S. anglica* and *S. maritima* located nearby, at the same topographic level and exposed to the same hydrodynamic conditions. The patches of the two *Spartina* species presented approximately the same characteristics, with a diameter of 2.5 m and plant height between 10 and 20 cm (variable with the season). They were placed approximately 20 m apart and located at about 250 m from the shoreline. At the center of the two selected patches (one of each species), we positioned an ALTUS probe [58], consisting of an acoustic altimeter coupled to a pressure sensor to perform continuous measurements of the bed-level variation and associated wave events under the influence of each *Spartina* species (Figure 1b,d). We followed the protocol proposed by Ganthy et al. [50] for the use of ALTUS systems within vegetation. Given the constraints associated with instrument deployment, only one site was considered in this study. A long-term deployment was performed where bed-level measurements were collected for more than one year. Plants growing under the range of the ALTUS sensor were cut at the beginning of the experiment, and the need of plant trimming was monitored at every site inspection. Bed-level measurements within vegetation were previously performed by Ganthy et al. [50] where data collection under such conditions was validated.

ALTUS devices are submergible acoustic altimeters with 0.2 mm resolution and 5 mm accuracy [59]. Both water depth and sediment bed level data were acquired in bursts of 260 s, every 15 min at a frequency of 2 Hz, during immersion periods. Sediment bed level measurements are performed through the emission and reception of a 1 MHz acoustic wave. The sensor can record up to 4 beams (B1 to B4). Each one of these beams is based on a different threshold of the returned acoustic energy, which is a proxy of the degree of the bed level density. This allows the detection of an eventually layered sediment bed. More precisely, in the case of a bed composed of more fluid sediment over consolidated one, the beam with lowest return signal should detect the water/sediment interface, and the remaining beams progressively detect the deeper layers up to the consolidated bottom. In absence of bed layering, all beams should provide an equivalent distance to the bottom. Because altimetry measurements can be affected by the presence of particles in the

water column that can diffuse the beams return signal and originate spikes of anomalous data, here we consider the altimetry based on the maximum echo obtained through the calculation of the standard deviation over the despiked burst, following the standard deviation method described by Nidzieko and Ralston [60], initially applied to velocity measurements using Acoustic Doppler velocimeters (ADV).

Free surface water level measurements by the ALTUS pressure sensor are provided at a resolution of 20 mm. Skewness of water elevation ($\gamma$) was computed for each semi-diurnal tide according to Soulsby [61], following Equation (1):

$$\gamma = \frac{\mu_3}{\mu_2^{3/2}} \tag{1}$$

where the $m$-th moment about zero is defined by Equation (2):

$$\mu_m = \frac{1}{N-1} \sum_{1=1}^{N} (n_i)^m \tag{2}$$

where $N$ is the number of samples $n_i$ and, in particular for water level asymmetry, $n$ is given by the variation of the water level over time following Equation (3):

$$n = \frac{\partial h}{\partial t} \tag{3}$$

The skewness of water elevation was used as a proxy for tidal horizontal asymmetry in order to estimate the asymmetry of tidal currents at the study site, where $\gamma > 0$ indicates ebb-dominance (ebb currents stronger than flood currents), and $\gamma < 0$ indicates flood dominance (flood currents stronger than ebb currents).

Wave height and period were extracted from the high-frequency water depth measurements through spectral analysis. Wave height was computed as the spectral significant wave height, given by Equation (4)

$$Hmo = \sqrt{\bar{E}/(gp)} \tag{4}$$

where $\bar{E}$ is the average wave energy, $g$ the gravitation acceleration, and $\rho$ is the water density. Wave period was computed as the period of highest energy, Tp, where Tp $\approx 5\sqrt{Hm0}$.

Maximum wave orbital velocities ($U_b$) were then calculated through linear wave theory. Subsequent bottom shear stress estimations were based on the wave induced friction factor ($f_w$) from Equation (5), according to [62]:

$$\tau_w = \frac{1}{2} \times \rho_{water} \times f_w \times U_b{}^2 \tag{5}$$

where $\rho_{water}$ is the water density (kg m$^{-3}$) and $f_w$ is estimated according to Ariathurai and Arulanandan [63], as function of the quotient between half the fluid particle excursion at the bottom and the bed roughness length ($Z_0$), expressed by Equation (6):

$$f_w = 1.39 \times (A/Z_0)^{0.52} \tag{6}$$

and assuming the typical value of $Z_0$ for muddy sediments of 0.2 mm. This formulation of $f_w$ was chosen for its good fit within a broad range of flow and sediment conditions. The value of 0.2 mm is indicated by Soulsby [61] as the typical value for muddy sediments. Even though sediment from the two stations presented slight differences in sediment composition, these differences were small, and the same $Z_0$ was considered for both. Nevertheless, we do not exclude the possibility that further attention should be given to variations in the influence of the $Z_0$ value in the bed sediment dynamics within the two species of vegetation. However, given the magnitude of differences we observed in the sediment dynamics patterns within

the two vegetation species, even with the assumption of the same bed roughness length for both stations; such analysis goes beyond the scope of the present study.

The total wave energy over each tidal cycle was estimated from Equation (7):

$$E_{wave} = \sum_{t-12}^{t} \frac{1}{8} \times 9.81 \times \rho_{water} \times H_{wave}(t)^2 \tag{7}$$

Considering that waves in the Bay are mainly wind generated, wind measurements (direction and intensity; Figure 1c) available at the meteorological station of Lège-Cap Ferret (Figure 1a) were used and directly correlated to wave direction. Atmospheric pressure data were also obtained to apply atmospheric and non-hydrostatic corrections to water depth measurements.

Surficial sediment samples were collected within the two meadows of *Spartina* in winter and summer to perform grain size analysis, water content and density determination.

Finally, since the two species may differently impact the state of bed sediments regarding erosion processes, we estimated the critical bottom shear stress for erosion ($\tau_{ce}$) from time-series of measured bed level and wave-4 erosion for both species. Ten events matching this criterion were found, with durations ranging from one single tidal cycle up to five consecutive tides. For each selected event, we applied the Partheniades erosion law given by Equation (8):

$$E(t) = E_0 \times \left( \frac{\tau_w(t)}{\tau_{ce}} - 1 \right) \text{ for } \tau_w > \tau_{ce}, \text{ and } E(t) = 0 \text{ for } \tau_w <= \tau_{ce} \tag{8}$$

where $E_0$ is the erosion rate (kg m$^{-2}$ s$^{-1}$). According to Partheniades [64], $E_0$ varies between 0.005 and 0.015 kg m$^{-2}$ $^{-1}$s, so we have considered these two values to consider the lower and higher erosion rate cases. Based on a recent work [65], we determined $E$ values depending on the winter value of the sand fraction measured for both species, giving $4.06 \times 10^{-5}$ and $3.1 \times 10^{-5}$ kg m$^{-2}$ s$^{-1}$ for *S. anglica* and *S. maritima,* respectively. For each wave event and species, 1000 values of $\tau_{ce}$ were alternatively tested (ranging from 0.001 to 4.000 N/m$^2$), and the value providing the best theoretical bed level evolution compared with data were retained. This sediment transport equation was chosen among other possibilities for its simplicity and for its commonly suggested use in cohesive sediments [65]. From the Partheniades relationship [66], we could then estimate the theoretical bed evolution for each selected wave event following Equation (9):

$$Hbed_{theoretical}(t) = Hbed_{theoretical}(t-1) - dh(t) \tag{9}$$

where *dh* (m) corresponds to the eroded thickness between time $t-1$ and $t$ according to Equation (10):

$$dh(t) = dt \times \frac{E(t)}{\rho_{dry}} \tag{10}$$

where *dt* is the time step between measurements $t-1$ and $t$ (seconds), $\rho_{dry}$ is the dry density of bed sediment (kg m$^{-3}$), and *E(t)* is the instantaneous erosion sediment flux, previously obtained through Equation (8). It is to note that the instantaneous erosion fluxes correspond to values averaged over the sampling time (260 s), and data were sampled every 15 min. This translates into timesteps of 20 min.

All correlations between hydrodynamic and sediment variation parameters were calculated through the Pearson correlation coefficient, with correlation significance threshold at $p > 0.5$.

## 3. Results

### 3.1. Seasonal to Event Patterns of Sediment Dynamics within S. anglica and S. maritima

Seasonal registered wave, sediment and vegetation characteristics for both stations are summarized in Table 1.

**Table 1.** Summary data for the two *Spartina* species stations. $\rho$ dry = sediments dry density; $\rho$ bulk = sediments bulk density; $D_{50}$ = Sediment mean particle size; Hm0 = mean spectral wave height (m); Hmax = maximum wave height (m); Tp = wave peak period (s); $\tau_w$ = Bed wave shear stress (N m$^{-2}$); h = water depth.

| Parameters | | *Spartina anglica* | | *Spartina maritima* | |
|---|---|---|---|---|---|
| | | **Autumn/Winter** | **Spring/Summer** | **Autumn/Winter** | **Spring/Summer** |
| **Plant properties** | Patch density (n° individuals m$^{-2}$ ±SE) | 39 (±8) | 63 (±13) | 124 (±16) | 130 (±24) |
| | Plant height (cm) | 15 | 15 | 20 | 20 |
| **Sediment properties** | Water content (%) | 188 (±60) | 216 (±23) | 224 (±20) | 218 (±15) |
| | $\rho$ dry (Kg m$^{-3}$) | 505 (±152) | 391 (±34) | 380 (±29) | 384 (±9) |
| | $\rho$ bulk (Kg m$^{-3}$) | 1363 (±90) | 1229 (±19) | 1226 (±25) | 1220 (±14) |
| | Porosity (−) | 0.86 (±0.06) | 0.84 (±0.02) | 0.85 (±0.02) | 0.84 (±0.01) |
| | D50 (μm) | 23.1 (±7.5) | 28.5 (±3.1) | 18.3 (±1.9) | 28.7 (±3.18) |
| | Fine sed. fraction (mud and silt %) | 81.3 (±11) | 73.6 (±4.7) | 87.5 (±1.9) | 74.7 (±4.4) |
| | Sand fraction (%) | 18.7 (±11) | 26.4 (±4.7) | 12.5 (±1.9) | 25.3 (±4.4) |
| **Hydrodynamics** | Hm0 (min, max) | <0.05, 0.65 | <0.05, 0.34 | <0.05, 0.63 | <0.05, 0.29 |
| | Hmax (min, max) | 0.06, 0.85 | 0.06, 0.38 | 0.05, 0.86 | 0.06, 0.33 |
| | Tp (min, max) | 1, 9 | 1, 9 | 1, 9 | 1, 9 |
| | $\tau_w$ (min, max) | 0.09, 16.42 | 0.1, 5.29 | 0.11, 15.12 | 0.16, 0.5 |
| | Hm0/h | 0.02, 0.27 | 0.02, 0.36 | 0.03, 0.47 | 0.08, 0.27 |

The hydrodynamic measurements showed differences between wave conditions during autumn/winter and spring/summer. Whereas during the low energy seasons wave heights were on average around 5 cm and did not exceed 20 cm, during the high energy seasons, wave heights varied between 5 cm and up to 65 cm, during periods of strong winds (Figure 2b). Even though wave heights within the two species of vegetation were of the same order of magnitude, with differences under 5 cm, they translated into different impacts on the bottom (Figure 2d). Notably, for the same wave events, wave bottom shear stress ($\tau_w$) was consistently higher by 4 to 30% within *Spartina anglica* than *Spartina maritima* stands (Figure 2c). In terms of plant specific characteristics, differences were mostly found in terms of patch density, where *S. maritima* density was twice higher than *Spartina anglica* during summer and their difference tripled in wintertime. This is likely a central factor explaining the differences observed within the hydrodynamics within the two *Spartina* species.
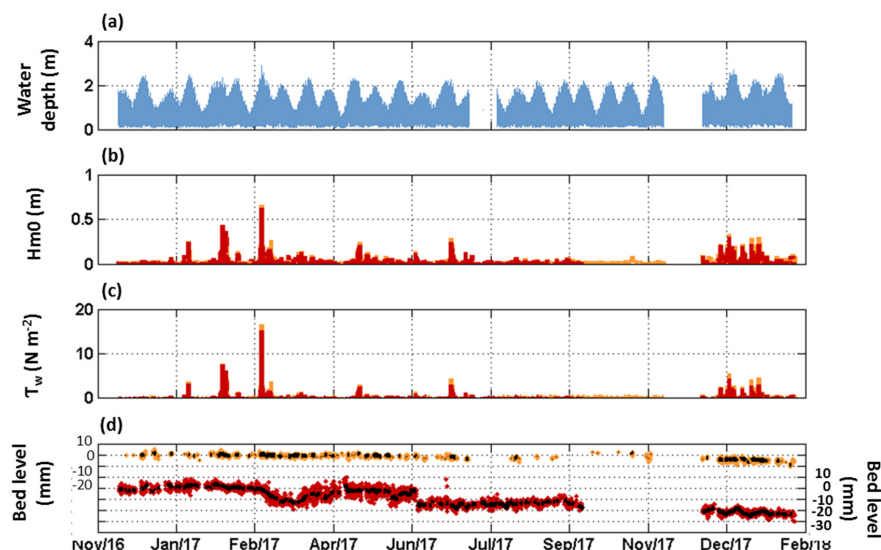


**Figure 2.** Time-series records of (**a**) water level, (**b**) spectral wave height for *Spartina anglica* station (yellow) and *Spartina maritima* (red) station, (**c**) wave bottom shear stress for S. anglica station (yellow) and *S. maritima* (red) station and (**d**) bed level variation within *S. anglica* (yellow–left axis) and *S. maritima* (red–right axis) and tide average bed level variation for both species (black line), for the entire survey period, between 28 November 2016 and 3 February 2018.

The comparison between the critical bed shear stress for erosion between the two *Spartina* species (Figure 3) showed that higher values (up to 3 times) of wave bed shear stress are required for sediment mobilization within the exotic *S. anglica* which is consistent with the lower bed level variability verified within the stands of this species.
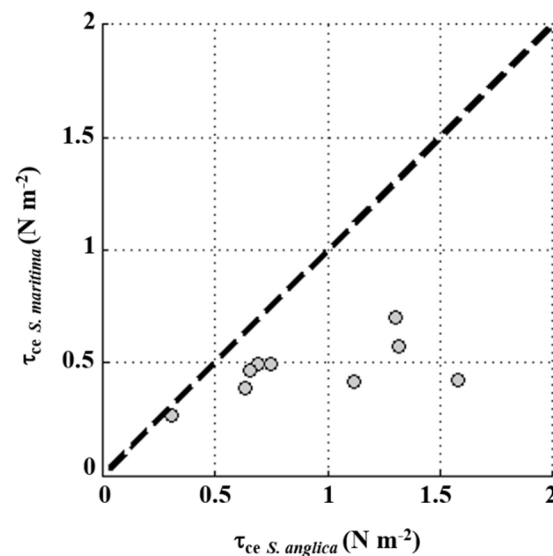


**Figure 3.** Critical bottom shear stress for erosion ($\tau_{ce}$—N m$^{-2}$) within *Spartina anglica* versus *Spartina maritima* ($p < 0.002$ with significance threshold at $p = 0.05$).

However, the analysis of wave action over the bed, both through its energy and wave bed shear stress, did not reveal a clear tendency in terms of bed level response within the two *Spartina* species (data not shown).

Sediment characteristics within the meadows of the two *Spartina* species were similar for the spring/summer period. Overall, both species presented a sediment characterized by medium silt, and during the low energy season, mean sediment grain size was 28 μm for the two species. Still under low energy conditions, both fine sediment and sand fractions presented close values, around 74% and 25%, respectively. However, differences between the two species increased during the high energy season (autumn/winter). Precisely, sediment in *S. maritima* showed higher percentage of fine sediments (6%), and conversely, sand percentage was lower by 6% than in the exotic *Spartina*. This translated in a slightly higher median sediment grain size (D50), with 23.1 μm against 18.3 μm, for the exotic species. Dry sediment density ($\rho_{dry}$) was also significantly different for the two species within this season, when sediment under the influence of *S. anglica* presented a $\rho_{dry}$ of 505 kg m$^{-3}$ whereas within *S. maritima* $\rho_{dry}$ was 384 kg m$^{-3}$ (Table 1).

Considering the seasonal sediment budget, presented in Figure 4, we observed that the sediment trapping capacity of the two species in the tidal flat during the survey period was strongly counterbalanced by the erosive processes as both species presented overall negative sediment budget, except for the spring/summer season within *Spartina anglica* that presented an accretion of 2.5 mm. Comparing the two autumn/winter seasons, we verified a strong inversion in the sediment budget in the behavior of the bed level between the two species explaining the contrasting net budget observed during the two winter periods in Figure 5. During autumn/winter 2016/2017, characterized by two spaced but stronger wave episodes, *Spartina maritima* presented a higher erosive behavior. During the second autumn/winter (2017/2018), wave events did not reach the same magnitudes as the previous one and the wave induced bottom shear stresses were more frequently above 1 N m$^{-2}$, comparing to the previous year. With this continuous action of waves, it was the bottom under the influence of *S. anglica* that presented higher sediment loss. However, the total budget indicates an erosion twice higher within *S. maritima* than *S. anglica* (Figure 4).
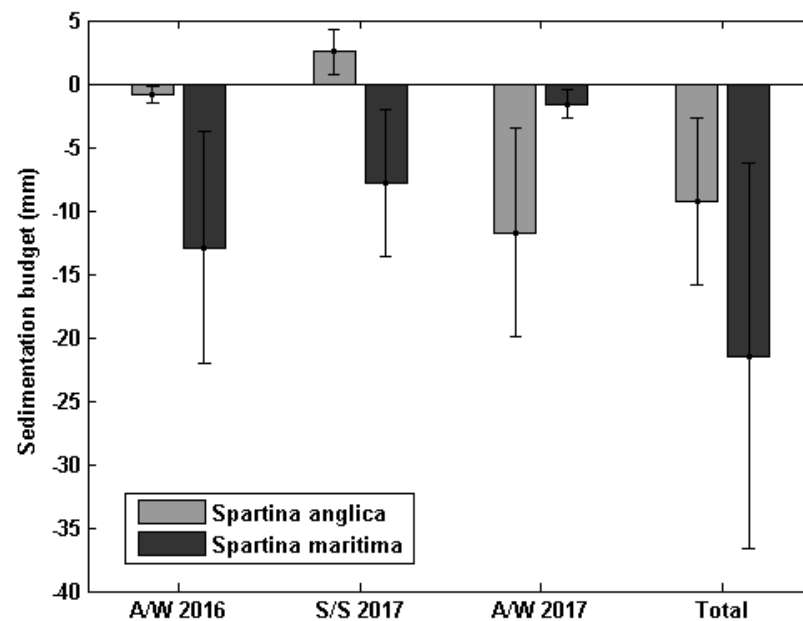
**Figure 4.** Sedimentation budget (mm) per season (A/W—autumn/winter and S/S—spring/summer) estimated from the difference in the bed level at the beginning and at the end of each season and total budget estimated from the difference in bed level between the beginning and the end of the survey. Negative values indicate erosion and positive values indicate accretion. Error bars represent standard deviation.

The evolution of the consolidation state of surficial sediment within the two *Spartina* species presented both seasonal and event related patterns (Figure 6). Notably, between mid-March and mid-June, during the low energy season, the thickness of the non-consolidated bed (soft mud layer) tended to be higher than during more energetic periods, in particular within *S. maritima*, where it ranged from under 5 mm up to around 1 cm, whereas within *S. anglica* the variation was always under 5 mm. During storm events, in particular the one of the 28 February 2017, within *S. maritima*, we observed a strong erosion, with a decrease of the consolidated bed of more than 1 cm. However, this did not produce an effective erosion of this order of magnitude as it was accompanied by a liquefaction of the upper layer of the bed, translated into an increase the soft mud layer thickness. The same behavior was found for *S. anglica* with variations of lower magnitude.
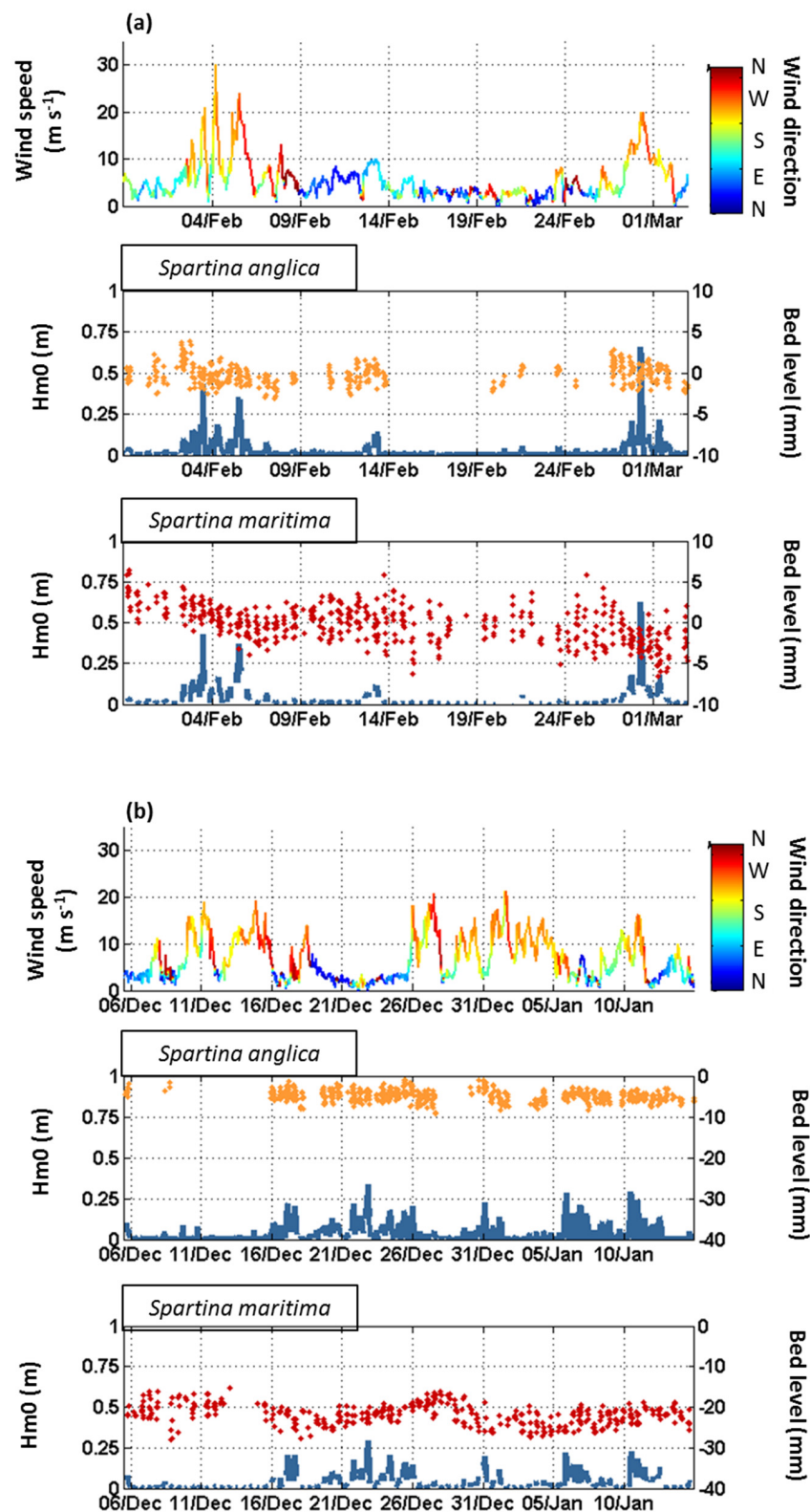
**Figure 5.** Zoom on winter storm events from (**a**) autumn/winter 2016 and (**b**) autumn/winter 2017. Top graphics consider wind conditions measured at Cap Ferret's meteorological station with wind speed (line representation) and wind direction (color representation). Central graphics represent measured mean wave height (blue line) and bed level variation (yellow dots) under the influence of *Spartina anglica*. Bottom graphics represent measured mean wave height (blue line) and bed level variation (red dots) under the influence of *Spartina maritima*.
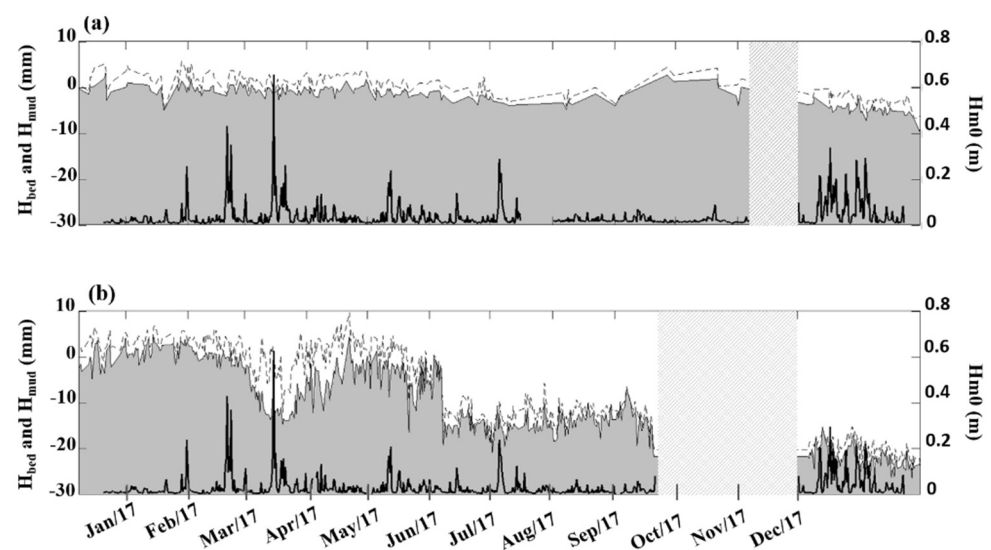
**Figure 6.** Consolidated bed level (solid grey surface) and soft mud level (dashed black line) and corresponding mean wave height (black line) within the vegetation patches of (**a**) *Spartina anglica* and (**b**) *Spartina maritima*. Dashed grey box indicates "no data" period.

*3.2. Tide-Induced Variations in Sediment Dynamics*

As expressed by the long-term time series of bed level-change under the action of both *Spartina* species, tide-induced bed level dynamics showed the same behavior (well correlated accretion and erosion episodes) but with variations within *S. maritima* twice higher that within *S. anglica* (Figure 7).
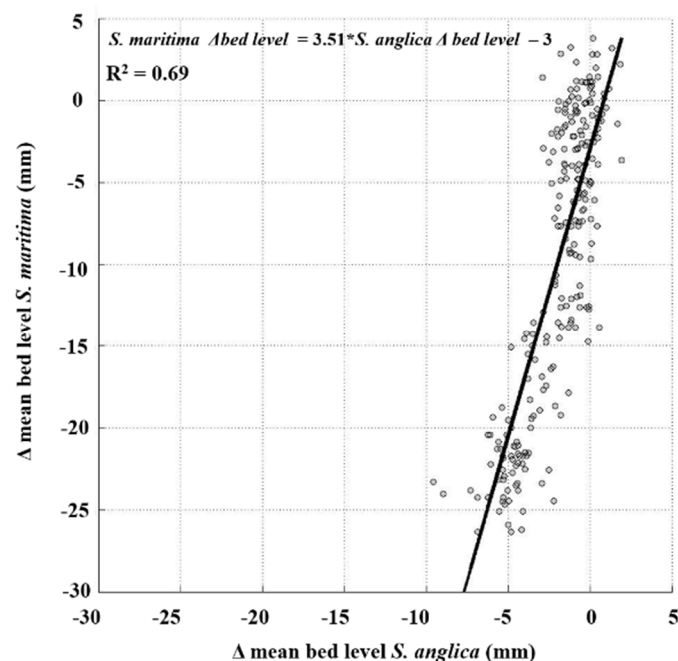


**Figure 7.** Bed level variation (in mm) within *Spartina maritima* versus variations within *Spartina anglica* vegetation. Bed level variations are tidally averaged values. Negative values indicate erosion, and positive values indicate accretion. Black line corresponds to linear regression expressed by the equation $y = 3.51x - 3$ ($R^2 = 0.83$, n = 235, $p < 0.001$, with significance threshold at $p = 0.05$).

The tidal asymmetry ($\gamma$) was found to increase with tidal range (Figure 8). The scatterplot indicates that the tide is ebb dominant for neap tides, while it becomes flood dominant for spring tides, above a tidal range of approximately 1.2 m. The linear increase in flood

dominance with tidal range can favor sediment import into the study site for spring tides conditions. More precisely, during spring tides, when currents are stronger, more sediment is likely to be eroded from channels and tidal flats and because flood currents are stronger (flood dominance), sediment transport occurs mostly towards the inner Bay where it settles with lower probability of being re-suspended in ebb due to weaker currents. Conversely, during neap tides, when ebb currents exceed flood currents, sediment is more likely to be re-suspended and mobilized from the site.
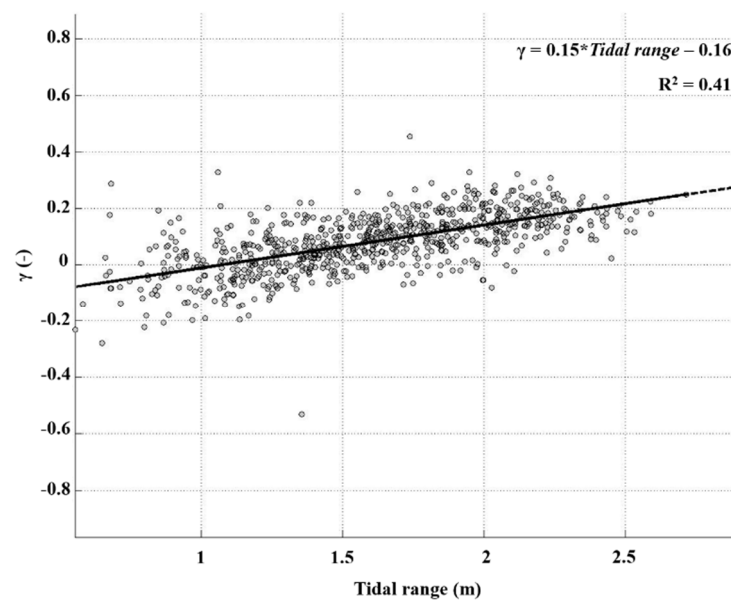


**Figure 8.** Tidal asymmetry index ($\gamma$) as a function of tidal range (m) at the study site. Black line corresponds to linear regression expressed by the equation $y = 0.15x - 0.16$ ($R^2 = 0.41$, n = 778, $p < 0.001$ with significance threshold at $p = 0.05$). Values of $\gamma > 0$ correspond to flood dominance, and values of $\gamma < 0$ correspond to ebb dominance.

The sediment trapping efficiency of the two species can be verified by the estimation of the sedimentation rate at the two sites. The relationship between sedimentation rate and tidal range variation (Figure 9) showed strong correlation for the exotic *Spartina* ($R^2 = 0.8$, $p < 0.001$) and no correlation for the native *Spartina* ($R^2 = 0.08$, $p < 0.001$), significant in both cases. Within *Spartina anglica*, a clear trend for accretion was verified (sedimentation rate > 0) in the transition from spring to neap tides (tidal range variation < 0). This is consistent with the previously indicated higher sediment availability during spring tides that can settle with decreasing tidal currents as we move towards a neap tide regime. In the transition from neap to spring tides, a tendency for erosion was found instead, mostly related to the increase in tidal current velocities that will then re-suspend sediment that previously settled. Sediment variation within *Spartina maritima* influence showed a lower direct response to this tidal regime.
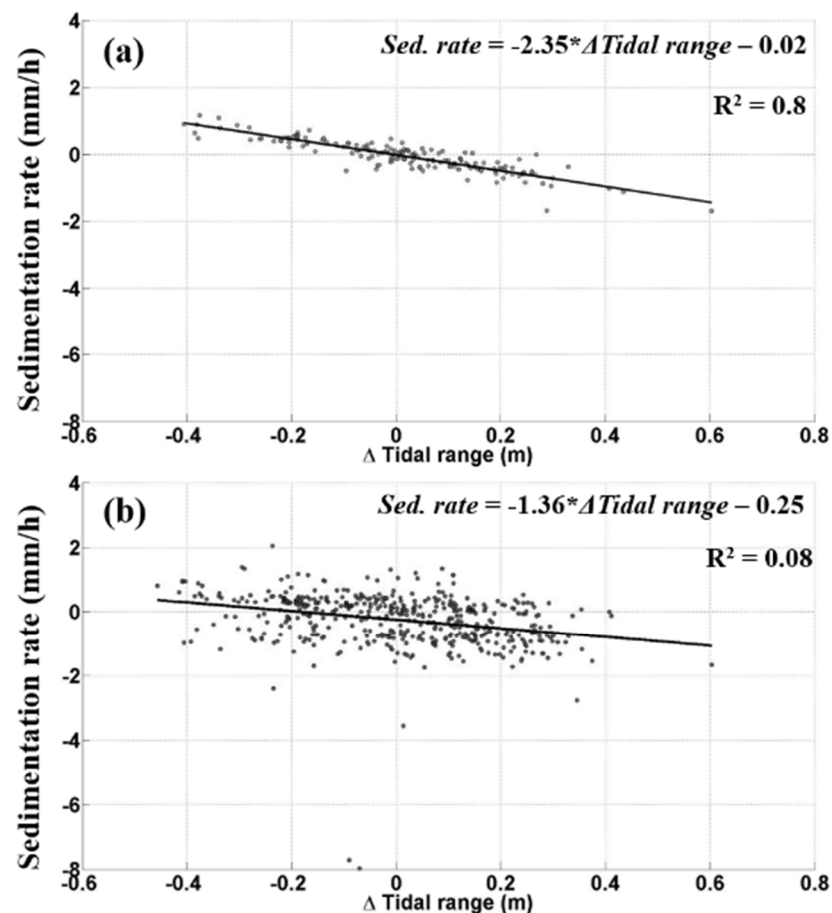
**Figure 9.** Sedimentation rate (mm h$^{-1}$) as a function of tidal range variation within (**a**) *Spartina anglica* and (**b**) *Spartina maritima*. Solid line corresponds to linear regression expressed by the equations y = −2.35x − 0.02 (R$^2$ = 0.8, n = 168, *p* < 0.001) for *S. anglica* and y = −1.36x − 0.25 (R$^2$ = 0.08, n = 472, *p* < 0.001) for *S. maritima* (with significance threshold at *p* = 0.05).

### 3.3. Annual Bed Level Evolution under Spartina Influence

The hydrodynamic measurements for the whole time series (Figure 2a,c) showed that the two considered winters presented overall different energetic conditions. Notably, the autumn/winter 2016/2017 was marked by strong episodic storm events where wave heights and wave bed shear stress reached around 0.85 m and 16 N m$^{-2}$, respectively, whereas autumn/winter 2017/2018 was characterized by longer and lower magnitude wave events where wave heights and wave bed shear stresses did not go over 0.4 m and 5 N m$^{-2}$, respectively.

The observations of the long-term time series (whole period of survey) revealed a general stronger tendency for sediment stability under the influence of the exotic *S. anglica* than the native *S. maritima*, both under calm and energetic hydrodynamic conditions (Figure 2d). The bed level within the exotic *Spartina* patch experienced little change, presenting variations within an amplitude of 5 mm. On the other hand, inside the patch of the native *S. maritima*, the amplitude of bed level change was considerably larger, not only on a regular basis, with variations going up to ± 1 cm but also in response to particular wave events, like the storm from the 4th February 2017 (Figure 2b,c), presenting a net total decrease in bed level of 2.4 cm. Although, it is to note that the abrupt decrease in the bed level within *S. maritima* registered in June is not associated to any meaningful physical event but most likely to a field survey where vegetation under the sensor was trimmed hence possibly releasing soft sediment deposits. However, average bed level evolution within the two *Spartina* species was strongly correlated (R = 0.83—Figure 7), which indicates that the same processes govern sediment patterns within both species of

vegetation, i.e., that erosion and accretion occurred simultaneously for both species as response to the hydrodynamic forcing. Bed-level variations we measured were in the same order of magnitude as similar ALTUS measurements previously performed within seagrass meadows in the Bay of Arcachon by Ganthy et al. [50].

## 4. Discussion

With the present study, we observed strong differences in bed level dynamics between *Spartina anglica* and *Spartina maritima*, where, overall, sediment influenced by the exotic *Spartina* had a higher temporal stability than those influenced by the native species.

### 4.1. Sediment Dynamics under the Influence of Waves

In tidal flats, waves are considered as a primary driver for sediment dynamics [67,68], and the two considered *Spartina* species presented distinct magnitudes of response to energetic wave events. However, in both cases, a time shift was observed between the highest wave action and the starting time of erosion. Indeed, the first impact of wave action, rather than immediate sediment mobilization, is the liquefaction of the sediment bed, i.e., the oscillatory pressure generated by the incident waves on a consolidated bed level induces a fluidization of the surficial bed sediments that then become erodible and available for mobilization at the subsequent wave incidences [69]. Such process is consistent with our measurements of surficial mud layer thickness that showed, for the two species, an increase in the non-consolidated bed thickness at the arrival of energetic wave events, in particular for the native *S. maritima*. This higher fluidization within the native *Spartina* translated in higher erosion rate than within *Spartina anglica*. The sediment colonized by the native *Spartina* presented lower critical bottom shear stresses, which can be explained by less consolidated sediments. This may be due to the high sediment trapping capacity and consequent high bed level variability. In this case, a less dense root system can also contribute to a lower impact on sediment bed resistance to erosion. It is to note that the bottom shear stress estimation here considered (Equation (5)) does not consider the effect of unsteady flow. On one hand, the presence of dense canopies typically induces strong damping both in currents and waves due to the biologically increased bottom friction [24]. On the other hand, in the presence of vegetation stems and leaves, the Reynolds numbers typically range between values corresponding to unsteady flow conditions [16]. However, due to the complexity of the vegetation structures, it is not always easy to characterize the turbulence field. Nevertheless, it can be assumed that within denser canopies the velocity is nearly constant, and the production of shear turbulence only becomes important very close to bed. In our study, we have used a simplified approach based on the bed shear stress, and the effects of turbulence within the two species should be further explored.

The higher resistance to erosion of sediments underneath the exotic *Spartina*, demonstrated by the higher critical wave shear stresses within its meadow, supports an increased bed consolidation within this species, probably related to its voluminous root system. Alternatively, the erosion differences found for the two species could be explained by the canopy density related turbulence. It has been experimentally shown by Tinoco and Coco [7] that higher plant density requires higher critical wave orbital velocity for sediment resuspension, but denser arrays of vegetation also increase turbulent kinetic energy levels. Consequently, it is turbulence and not wave orbital velocity that is the main driver for sediment resuspension because they found a decrease in wave orbital velocity in increased vegetation, and they still had high suspended sediment concentrations. Indeed, our meadows did show a substantial difference in terms of canopy density, but further hydrodynamic measurements should be performed in order to verify such findings.

Nevertheless, erosion events were always associated to the occurrence of storms and they were more intense for the sediment bed under the action of *Spartina maritima* than within *Spartina anglica*.

*4.2. Tidally Driven Sediment Dynamics*

The relationship between the sedimentation rate and tidal range variation within the two species of *Spartina* showed a much higher variability with tidal action within the native *S. maritima* than the exotic *S. anglica*. Sedimentation rates in tidal flats are directly linked with the duration of the tidal inundation [70]. Therefore, the tidal forcing action, which is the dominant forcing during summertime, when periods characterized by large waves are scarce, represents an important factor in the sediment trapping capacity of a particular species. Due to its denser canopy, the native *Spartina maritima* showed a stronger capacity for sediment trapping. However, freshly deposited sediments are more easily eroded than consolidated muddier sediments, and increased permeability and water content reduce soil strength and resistance to erosion [71]. Because *S. maritima* exhibits a strong ability for sediment trapping, new sediment is continuously depositing without time to get consolidated and is easily washed away. Such process was also verified by Ganthy et al. [40] within *Zostera noltei* meadows during the low energy summer season. On the other hand, the exotic *Spartina*, at the pioneer stage, presented sparse aerial surface coverage, which indicates that its action on flow deceleration and subsequent capacity for sediment trapping is probably limited, inducing less sediment motion variation. This suggests that at the earlier stage of development, the ecosystem-engineering ability of *Spartina anglica* to vertically increase soil elevation is mostly related to its high resistance to erosion and the organic contributions of vegetation [72], rather than by accumulation of inorganic sediment. Overall, tidally driven sediment dynamics mostly induced accretion at the site but it was of very low magnitude and, on the short term, was higher within the native *Spartina* canopy. Considering the combination between tides and episodic storm events, essential for the long-term dynamics, we verified that, on one hand, storms induce erosion, and on the other hand, tidal dominance during fair weather induces accretion. The weighing of these two processes indicates a stronger predominance of storm-induced erosion which, along with sediment supply deficiency within the inner zone of the Bay, leads to a general trend to bed erosion at the study site.

*4.3. Long-Term Differences in Bed Level Variation between S. anglica and S. maritima*

The seasonal continuous monitoring of bed level evolution under the action of the two species of *Spartina* revealed a species dependent influence on soil stabilization in the tidal flats. Biomass measurements of the two *Spartina* species in the Bay of Arcachon [43] have shown that, on the lower intertidal levels, the exotic *Spartina*, *S. anglica*, presents twice higher belowground allocation than aboveground whereas the native one, *S. maritima* favors aboveground biomass to the detriment of roots and rhizomes. The long-term variations in bed evolution we have registered within the two types of vegetation are consistent with this biomass distribution for the two *Spartina* species. The soil under the influence of the invasive *Spartina* presented considerable stability, even during the action of energetic hydrodynamic events. This capacity of voluminous root systems to increase soil resistance [6,32,37] to erodibility has particularly been shown by the works of Vanoppen et al. [39]. These authors verified an inter-specific effectiveness in reducing soil erosion rates and that resistance to erosion was positively correlated to root biomass density.

Strong ecosystem engineers in tidal flats, such as *Spartina* species, are most commonly known to enhance bed elevation [73]. This is valid for homogenous well-developed marshes. However, for isolated clone *Spartina* patches in the pioneer zone, it is not always the case, and the topographic evolution (expansion or shrinking) of the tussock strongly depends on the large-scale net-sediment dynamics, sediment grain size and other prevailing abiotic conditions that can change in time [32]. Indeed, the size of clone is considered as a major factor in conditioning accretion. References [74,75] have found an increase in accretion rates with increasing patch diameter for *Spartina maritima* population. In our study, we found a general tendency for sediment loss within the patches of the two species of *Spartina*. Considering that rivers are a major player in intertidal morphodynamics providing sediment for salt marsh expansion [6], this can possibly be due to the low

mineral sediment availability in the Bay of Arcachon. In fact, salt marshes maintain their elevation by deposition of mineral sediment and production of organic matter, but vertical and horizontal marsh growth is only possible if there is enough sediment available in the water column [6,35,70,76]. In this process, the tidal inundation is an important factor, and it can be considerably affected by changes in Sea Level Rise. The channel network at the entrance of the Bay has been giving signs that the lagoon is currently adapting to Sea Level Rise [77]. However, further studies should be performed to address the role of the salt marshes in the Bay to this adaptation.

### 4.4. Limitations

A different bed-level variation behavior induced by hydrodynamic forcing was observed within the exotic *Spartina anglica* and the native *Spartina maritima*. However, the methodology here described presents limitations to the generation of conclusive data regarding the two species impact on sediment stabilization. The characterization of the two *Spartina* species biomass allocation was extensively performed and presented in Proença et al. [43]. It showed a root/shoot ratio 30% higher for the exotic *Spartina* than the native one ($p < 0.001$). However, bed-level measurements were only possible to perform at one site which restraints the validation of within species variations. We considered pioneer marsh vegetation, which due to higher exposure to harsh hydrodynamic conditions (higher wave heights and longer inundation times) experiences stronger die-back of aboveground biomass during winter seasons than marsh plants located closer to the coast in denser patches. It is therefore possible that a different behavior could be observed with measurements at more landward located marsh zones, either due to more sheltered conditions or to more constant vegetation properties. Additionally, field replication of combined hydrodynamic and bed-level variation measurements within vegetation meadows presenting the same stage of development and exposed to the same physical forcing in the field is very difficult to achieve. The natural variability of the environment creates a spatial variability in the hydrodynamic conditions which limits the assessment of the intra-specific variability response. For this reason, in studies, such interactions between vegetation and physical parameters are commonly assessed under controlled laboratory conditions.

We have attributed the differences in bed-level responses to wave action to the biomass allocation of the two cordgrass species. For instance, the role of belowground biomass for reducing erosion is not straightforward to interpret and might be related to other variables that influence the erosion-sedimentation rates [78]. An integrated assessment considering not only plant biomass but also sediment composition including the presence of benthic organisms would be desirable.

Given the abovementioned limitations further investigation could provide more conclusive insights on the biomass allocation influence on bed-sediment stabilization. This could be achieved not only with a similar field experiment considering more replicates of coupled hydrodynamic and bed-level measurements per species but also with controlled laboratory erodimetry experiments. Still, the data here presented provide verifiable field data showing different bed-level variation behaviors within the two species.

### 5. Conclusions

The understanding of vegetation related short-term tidal flat sediment dynamics is essential to the knowledge of the species' dependent long term cyclic processes of marsh development. Since salt marshes play a coastal protection role, this knowledge becomes important in a context of global change, where storm intensity and frequency are predicted to increase [79].

The monitoring of bed level variation under the influence of the invasive *Spartina anglica* showed weak erosion both on the event scale (response to storms) and on the long-term in opposition to *Spartina maritima* that presented much higher vulnerability for sediment loss during high energy events. However, the exotic species also showed a limited ability in promoting accretion on the pioneer zone of the mudflat comparing to

the native one. The joint action of these two effects seems to lead to a more effective bed stabilization and protection against erosion from the exotic *Spartina anglica*, pointing out this species as a better ecosystem engineer on the mudflat's pioneer zone.

Our measurements suggest that closely related species can present different influences on sedimentation/erosion patterns which should be considered within management actions. Due to the logistic constraints of instrument deployment that did not allow a spatial replication of our study, we are aware that inter-species differences are not quantified statistically and conclusions are mostly qualitative. Hence, care needs to be taken in drawing generalized conclusions. However, the long period of data collection of our study that enabled to capture two consecutive winter seasons showed a consistent behavior between seasons for both species and highlights the need of further investigation on species dependency bed stabilization to consolidate our observations. Such knowledge on the species ability to promote marsh expansion is important to mitigate global change effects and help in the preservation of salt marshes. Additionally, in a context where marshes are globally being threatened by human action [13,80], it is important to understand the different species' adaptation mechanisms to the environment they colonize as well as the repercussions these biologically induced changes can have on a global scale and with an interdisciplinary perspective in order to achieve a balanced evaluation of eventual coastal management measures that should be taken.

# References

1. D'Alpaos, A.; Lanzoni, S.; Marani, M.; Rinaldo, A. Landscape evolution in tidal embayments: Modeling the interplay of erosion, sedimentation, and vegetation dynamics. *J. Geophys. Res. Space Phys.* **2007**, *112*. [CrossRef]
2. Kirwan, M.L.; Murray, A.B. A coupled geomorphic and ecological model of tidal marsh evolution. *Proc. Natl. Acad. Sci. USA* **2007**, *104*, 6118–6122. [CrossRef]
3. Temmerman, S.; Bouma, T.; Van De Koppel, J.; Van Der Wal, D.; De Vries, M.; Herman, P. Vegetation causes channel erosion in a tidal landscape. *Geology* **2007**, *35*, 631–634. [CrossRef]
4. Murray, A.B.; Knaapen, M.A.F.; Tal, M.; Kirwan, M.L. Biomorphodynamics: Physical-biological feedbacks that shape landscapes. *Water Resour. Res.* **2008**, *44*. [CrossRef]
5. Bouma, T.; Temmerman, S.; van Duren, L.; Martini, E.; Vandenbruwaene, W.; Callaghan, D.; Balke, T.; Biermans, G.; Klaassen, P.; van Steeg, P.; et al. Organism traits determine the strength of scale-dependent bio-geomorphic feedbacks: A flume study on three intertidal plant species. *Geomorphology* **2013**, *180–181*, 57–65. [CrossRef]

6. Fagherazzi, S.; Mariotti, G.; Wiberg, P.; McGlathery, K. Marsh Collapse Does Not Require Sea Level Rise. *Oceanography* **2013**, *26*, 70–77. [CrossRef]

7. Tinoco, R.O.; Coco, G. Turbulence as the Main Driver of Resuspension in Oscillatory Flow Through Vegetation. *J. Geophys. Res. Earth Surf.* **2018**, *123*, 891–904. [CrossRef]

8. Coco, G.; Zhou, Z.; van Maanen, B.; Olabarrieta, M.; Tinoco, R.; Townend, I. Morphodynamics of tidal networks: Advances and challenges. *Mar. Geol.* **2013**, *346*, 1–16. [CrossRef]

9. Hu, Z.; Willemsen, P.W.J.M.; Borsje, B.W.; Wang, C.; Wang, H.; van der Wal, D.; Zhu, Z.; Oteman, B.; Vuik, V.; Evans, B.; et al. Synchronized high-resolution bed-level change and biophysical data from 10 marsh–mudflat sites in northwestern Europe. *Earth Syst. Sci. Data* **2021**, *13*, 405–416. [CrossRef]

10. Borsje, B.W.; van Wesenbeeck, B.K.; Dekker, F.; Paalvast, P.; Bouma, T.J.; van Katwijk, M.M.; de Vries, M.B. How ecological engineering can serve in coastal protection. *Ecol. Eng.* **2011**, *37*, 113–122. [CrossRef]

11. Temmerman, S.; Meire, P.; Bouma, T.J.; Herman, P.M.J.; Ysebaert, T.; De Vriend, H.J. Ecosystem-based coastal defence in the face of global change. *Nature* **2013**, *504*, 79–83. [CrossRef] [PubMed]

12. Ondiviela, B.; Losada, I.J.; Lara, J.L.; Maza, M.; Galván, C.; Bouma, T.J.; Van Belzen, J. The role of seagrasses in coastal protection in a changing climate. *Coast. Eng.* **2014**, *87*, 158–168. [CrossRef]

13. Barbier, E.B.; Hacker, S.D.; Kennedy, C.; Koch, E.W.; Stier, A.C.; Silliman, B.R. The value of estuarine and coastal ecosystem services. *Ecol. Monogr.* **2011**, *81*, 169–193. [CrossRef]

14. Bouma, T.J.; De Vries, M.B.; Low, E.; Peralta, G.; Tánczos, I.C.; Van De Koppel, J.; Herman, P.M.J. Trade-offs related to ecosystem engineering: A case study on stiffness of emerging macrophytes. *Ecology* **2005**, *86*, 2187–2199. [CrossRef]

15. Bouma, T.J.; van Duren, L.A.; Temmerman, S.; Claverie, T.; Blanco-Garcia, A.; Ysebaert, T.; Herman, P.M.J. Spatial flow and sedimentation patterns within patches of epibenthic structures: Combining field, flume and modelling experiments. *Cont. Shelf Res.* **2007**, *27*, 1020–1045. [CrossRef]

16. Neumeier, U.; Amos, C.L. The influence of vegetation on turbulence and flow velocities in European salt-marshes. *Sedimentology* **2006**, *53*, 259–277. [CrossRef]

17. Nepf, H.M. Flow and Transport in Regions with Aquatic Vegetation. *Annu. Rev. Fluid Mech.* **2012**, *44*, 123–142. [CrossRef]

18. Ganthy, F.; Soissons, L.; Sauriau, P.-G.; Verney, R.; Sottolichio, A. Effects of short flexible seagrass Zostera noltei on flow, erosion and deposition processes determined using flume experiments. *Sedimentology* **2015**, *62*, 997–1023. [CrossRef]

19. Maza, M.; Lara, J.; Losada, I.; Ondiviela, B.; Trinogga, J.; Bouma, T. Large-scale 3-D experiments of wave and current interaction with real vegetation. Part 2: Experimental analysis. *Coast. Eng.* **2015**, *106*, 73–86. [CrossRef]

20. Weitzman, J.S.; Zeller, R.B.; Thomas, F.I.M.; Koseff, J.R. The attenuation of current- and wave-driven flow within submerged multispecific vegetative canopies. *Limnol. Oceanogr.* **2015**, *60*, 1855–1874. [CrossRef]

21. Losada, I.J.; Maza, M.; Lara, J.L. A new formulation for vegetation-induced damping under combined waves and currents. *Coast. Eng.* **2016**, *107*, 1–13. [CrossRef]

22. Nowacki, D.J.; Beudin, A.; Ganju, N.K. Spectral wave dissipation by submerged aquatic vegetation in a back-barrier estuary. *Limnol. Oceanogr.* **2017**, *62*, 736–753. [CrossRef]

23. Horstman, E.M.; Dohmen-Janssen, C.M.; Hulscher, S.J. Flow routing in mangrove forests: A field study in Trang province, Thailand. *Cont. Shelf Res.* **2013**, *71*, 52–67. [CrossRef]

24. Neumeier, U. Velocity and turbulence variations at the edge of saltmarshes. *Cont. Shelf Res.* **2007**, *27*, 1046–1059. [CrossRef]

25. Chen, Y.; Li, Y.; Cai, T.; Thompson, C.; Li, Y. A comparison of biohydrodynamic interaction within mangrove and saltmarsh boundaries. *Earth Surf. Process. Landf.* **2016**, *41*, 1967–1979. [CrossRef]

26. Temmerman, S.; Bouma, T.J.; Govers, G.; Wang, Z.B.; De Vries, M.; Herman, P.M.J. Impact of vegetation on flow routing and sedimentation patterns: Three-dimensional modeling for a tidal marsh. *J. Geophys. Res. Earth Surf.* **2005**, *110*. [CrossRef]

27. Chen, Y.; Cai, T.; Chang, Y.; Huang, S.; Xia, T. Comparison of Flow and Energy Reduction by Representative Intertidal Plants, Southeast China. In Proceedings of the Twenty-Eighth (2018) International Ocean and Polar Engineering Conference, Sapporo, Japan, 15 June 2018.

28. Bernik, B.M.; Eppinga, M.B.; Kolker, A.S.; Blum, M.J. Clonal Vegetation Patterns Mediate Shoreline Erosion. *Geophys. Res. Lett.* **2018**, *45*, 6476–6484. [CrossRef]

29. Peralta, G.; Van Duren, L.; Morris, E.; Bouma, T. Consequences of shoot density and stiffness for ecosystem engineering by benthic macrophytes in flow dominated areas: A hydrodynamic flume study. *Mar. Ecol. Prog. Ser.* **2008**, *368*, 103–115. [CrossRef]

30. Bouma, T.J.; Ortells, V.; Ysebaert, T. Comparing biodiversity effects among ecosystem engineers of contrasting strength: Macrofauna diversity in Zostera noltii and Spartina anglica vegetations. *Helgol. Mar. Res.* **2009**, *63*, 3–18. [CrossRef]

31. Green, M.O.; Coco, G. Review of wave-driven sediment resuspension and transport in estuaries-. *Rev. Geophys.* **2014**, *52*, 77–117. [CrossRef]

32. Balke, T.; Klaassen, P.C.; Garbutt, A.; van der Wal, D.; Herman, P.M.; Bouma, T.J. Conditional outcome of ecosystem engineering: A case study on tussocks of the salt marsh pioneer Spartina anglica. *Geomorphology* **2012**, *153–154*, 232–238. [CrossRef]

33. Fagherazzi, S.; Kirwan, M.L.; Mudd, S.M.; Guntenspergen, G.R.; Temmerman, S.; D'Alpaos, A.; Van De Koppel, J.; Rybczyk, J.M.; Reyes, E.; Craft, C.B.; et al. Numerical models of salt marsh evolution: Ecological, geomorphic, and climatic factors. *Rev. Geophys.* **2012**, *50*. [CrossRef]

34. Kirwan, M.L.; Megonigal, J.P. Tidal wetland stability in the face of human impacts and sea-level rise. *Nature* **2013**, *504*, 53–60. [CrossRef]
35. Friedrichs, C.T.; Perry, J.E. Tidal Salt Marsh Morphodynamics: A Synthesis. *J. Coast. Res.* **2001**, *SI 27*, 7–37.
36. Coops, H.; Geilen, N.; Verheij, H.J.; Boeters, R.; Van Der Velde, G. Interactions between waves, bank erosion and emergent vegetation: An experimental study in a wave tank. *Aquat. Bot.* **1996**, *53*, 187–198. [CrossRef]
37. Schwarz, M.; Lehmann, P.; Or, D. Quantifying lateral root reinforcement in steep slopes—From a bundle of roots to tree stands. *Earth Surf. Process. Landf.* **2010**, *35*, 354–367. [CrossRef]
38. Twomey, A.J.; Saunders, M.I.; Callaghan, D.P.; Bouma, T.J.; Han, Q.; O'Brien, K.R. Lateral sediment erosion with and without the non-dense root-mat forming seagrass Enhalus acoroides. *Estuarine Coast. Shelf Sci.* **2021**, *253*, 107316. [CrossRef]
39. Vannoppen, W.; Poesen, J.; Peeters, P.; De Baets, S.; Vandevoorde, B. Root properties of vegetation communities and their impact on the erosion resistance of river dikes. *Earth Surf. Process. Landf.* **2016**, *41*, 2038–2046. [CrossRef]
40. Ganthy, F.; Sottolichio, A.; Verney, R. The Stability of Vegetated Tidal Flats in a Coastal Lagoon Through Quasi In-Situ Measurements of Sediment Erodibility. *J. Coast. Res.* **2011**, *SI 64*, 1500–1504.
41. Willemsen, P.W.J.M.; Borsje, B.W.; Hulscher, S.J.M.H.; Van Der Wal, D.; Zhu, Z.; Oteman, B.; Evans, B.; Möller, I.; Bouma, T.J. Quantifying Bed Level Change at the Transition of Tidal Flat and Salt Marsh: Can We Understand the Lateral Location of the Marsh Edge? *J. Geophys. Res. Earth Surf.* **2018**, *123*, 2509–2524. [CrossRef]
42. Baumel, A.; Ainouche, M.L.; Levasseur, J.E. Molecular investigations in populations of Spartina anglica C.E. Hubbard (Poaceae) invading coastal Brittany (France). *Mol. Ecol.* **2001**, *10*, 1689–1701. [CrossRef]
43. Proença, B.; Nez, T.; Poli, A.; Ciutat, A.; Devaux, L.; Sottolichio, A.; Montaudouin, X.; Michalet, R. Intraspecific facilitation explains the spread of the invasive engineer Spartina anglica in Atlantic salt marshes. *J. Veg. Sci.* **2019**, *30*, 212–223. [CrossRef]
44. Bouma, T.J.; Van Belzen, J.; Balke, T.; Van Dalen, J.; Klaassen, P.; Hartog, A.M.; Callaghan, D.P.; Hu, Z.; Stive, M.J.F.; Temmerman, S.; et al. Short-term mudflat dynamics drive long-term cyclic salt marsh dynamics: Lateral Salt Marsh Dynamics. *Limnol. Oceanogr.* **2016**, *61*, 2261–2275. [CrossRef]
45. Plus, M.; Dumas, F.; Stanisière, J.-Y.; Maurer, D. Hydrodynamic characterization of the Arcachon Bay, using model-derived descriptors. *Cont. Shelf Res.* **2009**, *29*, 1008–1013. [CrossRef]
46. Allard, J.; Chaumillon, E.; Fenies, H. A synthesis of morphological evolutions and Holocene stratigraphy of a wave-dominated estuary: The Arcachon lagoon, SW France. *Cont. Shelf Res.* **2009**, *29*, 957–969. [CrossRef]
47. Parisot, J.-P.; Diet-Davancens, J.; Sottolichio, A.; Crosland, E.; Drillon, C.; Verney, R. Modélisation des agitations dans le bassin d'Arcachon. *Xèmes Journées Nationales Génie Côtier—Génie Civil JNGCGC* **2008**, 435–444. [CrossRef]
48. Cayocca, F. Long-term morphological modeling of a tidal inlet: The Arcachon Basin, France. *Coast. Eng.* **2001**, *42*, 115–142. [CrossRef]
49. Salles, P.; Sottolichio, A.; Sénéchal, N.; Valle-Levinson, A. Wind-driven modifications to the residual circulation in an ebb-tidal delta: Arcachon Lagoon, Southwestern France-Salles-2015. *J. Geophys. Res. Oceans* **2015**, *120*, 728–740. [CrossRef]
50. Ganthy, F.; Sottolichio, A.; Verney, R. Seasonal modification of tidal flat sediment dynamics by seagrass meadows of Zostera noltii (Bassin d'Arcachon, France). *J. Mar. Syst.* **2013**, *109–110*, S233–S240. [CrossRef]
51. Martin, P.; Sébastien, D.; Gilles, T.; Auby, I.; de Montaudouin, X.; Emery, É.; Claire, N.; Christophe, V. Long-term evolution (1988–2008) of *Zostera* spp. meadows in Arcachon Bay (Bay of Biscay). *Estuar. Coast. Shelf Sci.* **2010**, *87*, 357–366. [CrossRef]
52. Blanchet, H.; De Montaudouin, X.; Chardy, P.; Bachelet, G. Structuring factors and recent changes in subtidal macrozoobenthic communities of a coastal lagoon, Arcachon Bay (France). *Estuar. Coast. Shelf Sci.* **2005**, *64*, 561–576. [CrossRef]
53. Kombiadou, K.; Ganthy, F.; Verney, R.; Plus, M.; Sottolichio, A. Modelling the effects of Zostera noltei meadows on sediment dynamics: Application to the Arcachon lagoon. *Ocean Dyn.* **2014**, *64*, 1499–1516. [CrossRef]
54. Costanza, R.; Pérez-Maqueo, O.; Martinez, M.L.; Sutton, P.; Anderson, S.J.; Mulder, K. The value of coastal wetlands for hurricane protection. *AMBIO* **2008**, *37*, 241–248. [CrossRef]
55. Cognat, M.; Ganthy, F.; Auby, I.; Barraquand, F.; Rigouin, L.; Sottolichio, A. Environmental factors controlling biomass development of seagrass meadows of Zostera noltei after a drastic decline (Arcachon Bay, France). *J. Sea Res.* **2018**, *140*, 87–104. [CrossRef]
56. Strong, D.R.; Ayres, D.R. Ecological and Evolutionary Misadventures of Spartina. *Annu. Rev. Ecol. Evol. Syst.* **2013**, *44*, 389–410. [CrossRef]
57. Proença, B.; Romuald, M.; Auby, I.; Ganthy, F.; Sottolichio, A.; Michalet, R. Disentangling ecosystem engineering from short-term biotic effects of a strong invader on a native foundation species. *Mar. Ecol. Prog. Ser.* **2019**, *621*, 69–81. [CrossRef]
58. Bassoullet, P.; Le Hir, P.; Gouleau, D.; Robert, S. Sediment transport over an intertidal mudflat: Field investigations and estimation of fluxes within the "Baie de Marenngres-Oleron" (France). *Cont. Shelf Res.* **2000**, *20*, 1635–1653. [CrossRef]
59. Jestin, H.; Bassoulet, P.; Le Hir, P.; L'Yavanc, J.; Degres, Y. Development of ALTUS, A High Frequency Acoustic Submersible Recording Altimeter to Accurately Monitor Bed Elevation and Quantify Deposition or Erosion of Sediments. In Proceedings of the IEEE Oceanic Engineering Society. OCEANS'98. Conference Proceedings (Cat. No.98CH36259), Nice, France, 28 September–1 October 1998; IEEE: Nice, France, 1998.
60. Cea, L.; Puertas, J.; Pena, L. Velocity measurements on highly turbulent free surface flow using ADV. *Exp. Fluids* **2007**, *42*, 333–348. [CrossRef]

61. Nidzieko, N.J.; Ralston, D.K. Tidal asymmetry and velocity skew over tidal flats and shallow channels within a macrotidal river delta. *J. Geophys. Res. Ocean.* **2012**, *117*. [CrossRef]
62. Soulsby, R.L. *Dynamics of Marine Sands*; Thomas Telford: London, UK, 1997.
63. Soulsby, R.L. *Modelling of Coastal Processes*; Thomas Telford: London, UK, 1993; pp. 111–118.
64. Ariathurai, R.; Arulanandan, K. Erosion Rates of Cohesive Soils. *J. Hydraul. Div.* **1978**, *104*, 279–283. [CrossRef]
65. Mengual, B.; Le Hir, P.; Cayocca, F.; Garlan, T. Modelling Fine Sediment Dynamics: Towards a Common Erosion Law for Fine Sand, Mud and Mixtures. *Water* **2017**, *9*, 564. [CrossRef]
66. Partheniades, E. Erosion and Deposition of Cohesive Soils. *J. Hydraul. Div. (ASCE)* **1965**, *91*, 105–139. [CrossRef]
67. Hu, Z.; Wang, Z.B.; Zitman, T.J.; Stive, M.J.F.; Bouma, T.J. Predicting long-term and short-term tidal flat morphodynamics using a dynamic equilibrium theory: Modeling Tidal Flat Dynamic Equilibrium. *J. Geophys. Res. Earth Surf.* **2015**, *120*, 1803–1823. [CrossRef]
68. Belliard, J.-P.; Silinski, A.; Meire, D.; Kolokythas, G.; Levy, Y.; Van Braeckel, A.; Bouma, T.J.; Temmerman, S. High-resolution bed level changes in relation to tidal and wave forcing on a narrow fringing macrotidal flat: Bridging intra-tidal, daily and seasonal sediment dynamics. *Mar. Geol.* **2019**, *412*, 123–138. [CrossRef]
69. Forsberg, P.; Ernstsen, V.; Andersen, T.; Winter, C.; Becker, M.; Kroon, A. The effect of successive storm events and seagrass coverage on sediment suspension in a coastal lagoon. *Estuar. Coast. Shelf Sci.* **2018**, *212*, 329–340. [CrossRef]
70. Kirwan, M.L.; Guntenspergen, G.R.; D'Alpaos, A.; Morris, J.T.; Mudd, S.M.; Temmerman, S. Limits on the adaptability of coastal marshes to rising sea level. *Geophys. Res. Lett.* **2010**, *37*. [CrossRef]
71. Escapa, M.; Perillo, G.M.; Iribarne, O. Sediment dynamics modulated by burrowing crab activities in contrasting SW Atlantic intertidal habitats. *Estuar. Coast. Shelf Sci.* **2008**, *80*, 365–373. [CrossRef]
72. Nyman, J.A.; Walters, R.J.; Delaune, R.D.; Patrick, W.H. Marsh vertical accretion via vegetative growth. *Estuar. Coast. Shelf Sci.* **2006**, *69*, 370–380. [CrossRef]
73. Thompson, J.D. The Biology of an Invasive Plant. What Makes Spartina Anglica so Successful? *BioScience* **1991**, *41*, 393–401. [CrossRef]
74. Castellanos, E.M.; Figueroa, M.E.; Davy, A.J. Nucleation and Facilitation in Saltmarsh Succession: Interactions between Spartina Maritima and Arthrocnemum Perenne. *J. Ecol.* **1994**, *82*, 239–248. [CrossRef]
75. Sanchez, J.; SanLeon, D.; Izco, J. Primary colonisation of mudflat estuaries by Spartina maritima (Curtis) Fernald in Northwest Spain: Vegetation structure and sediment accretion. *Aquat. Bot.* **2001**, *69*, 15–25. [CrossRef]
76. Lauzon, R.; Murray, A.B.; Moore, L.J.; Walters, D.C.; Kirwan, M.L.; Fagherazzi, S. Effects of Marsh Edge Erosion in Coupled Barrier Island-Marsh Systems and Geometric Constraints on Marsh Evolution. *J. Geophys. Res. Earth Surf.* **2018**, *123*, 1218–1234. [CrossRef]
77. Nahon, A.; Idier, D.; Sénéchal, N.; Féniès, H.; Mallet, C.; Mugica, J. Imprints of wave climate and mean sea level variations in the dynamics of a coastal spit over the last 250 years: Cap Ferret, SW France. *Earth Surf. Process. Landf.* **2019**, *44*, 2112–2125. [CrossRef]
78. Schoutens, K.; Heuner, M.; Minden, V.; Ostermann, T.S.; Silinski, A.; Belliard, J.-P.; Temmerman, S. How effective are tidal marshes as nature-based shoreline protection throughout seasons? *Limnol. Oceanogr.* **2019**, *64*, 1750–1762. [CrossRef]
79. Reguero, B.G.; Losada, I.J.; Méndez, F.J. A recent increase in global wave power as a consequence of oceanic warming. *Nat. Commun.* **2019**, *10*, 205. [CrossRef]
80. Doody, J.P. 'Coastal Squeeze'—An Historical Perspective. *J. Coast. Conserv.* **2004**, *10*, 129–138. [CrossRef]